Proc. Natl. Acad. Sci. USA
Vol. 77, No. 6, pp. 3360–3364, June 1980
Biochemistry

A proton-coupled conformational switch of *Escherichia coli* 5S ribosomal RNA

(5S RNA/RNA tertiary structure/RNA protonation/temperature-jump kinetics)

T. H. KAO AND D. M. CROTHERS

Department of Chemistry, Yale University, New Haven, Connecticut 06511

Communicated by Julian M. Sturtevant, March 24, 1980

ABSTRACT **We report temperature-jump kinetic studies of the early melting transition of *Escherichia coli* 5S rRNA. A single measurable relaxation time τ, independent of concentration, was found at 266 nm. We monitored the transition temperature t_m for this process (in the range from 0 to 40°C) as a function of Mg^{2+}, Na^+, K^+, spermidine, and H^+ concentrations. Contrary to the usual effect of salts on nucleic acid stability, addition of mono- and multivalent counterions decreases t_m for the early melting transition. Also unexpectedly, we found a strong dependence of t_m on pH in the physiological range of 7–8. Quantitative analysis of the data indicates that about 0.7 protons are released when the ordered (low-temperature) form melts, whereas about 2 Na^+ (or K^+) and 0.5 Mg^{2+} are taken up by the melted (high-temperature) form. We estimate the enthalpy of the transition to be 15–20 kcal/mol (63–84 kJ/mol) and also report the forward and reverse rate constants and activation energies for the transition, along with the influence of ions on the transition dynamics. Diffusion constant measurements reveal that the low-temperature form has a frictional coefficient about 10% larger than that of the high-temperature form. The data imply a low-temperature tertiary structure capable of binding a proton. Increase of pH, temperature, or counterion concentration (all at near-physiological values) causes a tertiary conformational switch to a more compact form that has greater counterion binding but less proton binding. We discuss possible physiological roles for the transition.**

The structure of *Escherichia coli* 5S rRNA has been studied by a wide variety of techniques, but a definitive model for its structure has yet to be obtained (1). Most proposed models deal only with 5S RNA secondary structure (2), but there is evidence from chemical reactivity (3), crosslinking (4), infrared spectroscopy (5), and conformational dynamic studies (6) for extensive tertiary structure. Furthermore, experience with other RNAs indicates a substantial dependence of structure on buffer conditions (7–10). Hence we decided to undertake a systematic study of conformational equilibria and dynamics in 5S RNA, using the temperature-jump method previously applied to tRNA (11–13). In this paper we present the results of our studies of the first, or early melting, transition, which has two unusual features: (*i*) The melting temperature decreases as Mg^{2+} or Na^+ (or K^+) concentration is raised. (*ii*) The melting temperature increases as the H^+ concentration is raised. On the basis of the kinetic, thermodynamic, and hydrodynamic data obtained from these studies we propose that the early melting transition reflects modification of a protonated tertiary structure, producing a more compact conformation.

The publication costs of this article were defrayed in part by page charge payment. This article must therefore be hereby marked "*advertisement*" in accordance with 18 U. S. C. §1734 solely to indicate this fact.

MATERIALS AND METHODS

Isolation and Purification of 5S RNA. Frozen *E. coli* MRE 600 cells (¾ through the logarithmic phase of growth) were purchased from Grain Processing Corporation (Muscatine, IA). Their 70S ribosomes were prepared according to Staehelin *et al.* (14). RNA was extracted with phenol and precipitated with ethanol at −20°C. RNA pellets were resuspended in TM buffer (10 mM Tris·HCl, pH 7.6/10 mM $MgCl_2$). An equal volume of 4 M NaCl (in TM buffer) was added and the solution was allowed to stand in ice overnight. The precipitate, mainly 23S and 16S RNA, was removed by low-speed centrifugation. The supernatant (5S RNA, tRNA, and some 16S RNA) was concentrated by rotational evaporation and loaded onto a Sephacryl S-200 column (2.5 × 100 cm) equilibrated with S-200 buffer (10 mM Tris·HCl, pH 7.6/10 mM $MgCl_2$/50 mM KCl/1% methanol). Chromatography was performed at room temperature. The flow rate was about 70 ml/hr. The fractions containing 5S RNA were pooled and stored at −20°C.

Analytical Gel Electrophoresis. The purity of 5S RNA was checked by 10% polyacrylamide gel electrophoresis as described by Weidner and Crothers (6). All the samples used for our physical studies were shown to be free of any detectable denatured 5S RNA (15).

Temperature-Jump Experiments. The temperature-jump instrument has been described in detail (16). The sample cell was constructed of Kel-F, with solid gold electrodes. The cell volume is 1.8 ml, with an optical path length of 0.7 cm. Samples (at concentrations ranging from 1 to 1.5 A_{260}) were filtered through a 0.22-μm-pore Milipore filter unit and degassed under suction. The temperature in the cell was measured with a YSI no. 611 thermistor probe (Yellow Springs Instrument) inserted into the upper electrode. A temperature jump of 3.76°C was produced by the discharge of a 0.05-μF capacitor charged to 20 kV. The relaxation signals were displayed on a Tektronix oscilloscope and stored in a Biomation model 802 transient recorder, which was interfaced to a PDP-11/40 digital computer. The transient signals were stored on floppy disk and later displayed on an oscilloscope for analysis by an interactive program culminating in a least-squares fitting calculation. The program, written by H. Neuwirth and M. Flam, is based on the Marquardt algorithm (17) and utilizes a combination of the method of steepest descents and the Newton–Raphson method. The rate of temperature increase for the melting experiments was approximately 5°/ hr. The absorbance change was monitored at 266 nm.

Laser Light-Scattering Experiments. The theories and instrumentation of laser light scattering experiments have been described (18, 19). Dynamic light scattering was performed by

using a Lexel argon ion laser (λ = 4880 Å) of 200–500 mW. The cell temperature was controlled at 11°C by circulating fluid. The autocorrelation function was generated in real time by a Malvern K7025 multi-bit correlator and the result was displayed on an oscilloscope. The signal was then fitted to a single exponential by a least-squares routine, with decay constant τ equal to $(2q^2D)^{-1}$, in which $q = (4\pi n/\lambda)\sin(\theta/2)$. All the measurements were done at $\theta = 90°$. Diffusion constants at 11°C were corrected for solvent viscosity to yield $D_{20,w}$.

RESULTS

5S RNA Shows an Early Melting Transition at 50 mM Na^+, 0.5 mM Mg^{2+}, and pH 7.45. We have observed four resolved melting transitions of *E. coli* 5S RNA between 0 and 90°C in a buffer containing 30 mM sodium cacodylate at pH 7.45, 20 mM $NaClO_4$, and 0.5 mM $MgCl_2$ (data not shown). We define the first transition (occurring between 10 and 40°C) as the early melting transition and focus on this transition in the present paper. Two relaxation effects were observed. The faster one, usually ascribed to base unstacking, occurred in the microsecond range or faster and could not be analyzed with our temperature-jump instrument. We have monitored the slower resolved relaxation effect, which occurs in the millisecond range. A semilogarithmic plot of the absorbance change from the resolved relaxation signal versus time gave a straight line within the noise level of the signal (root mean square noise level 3–10% of relaxation amplitude). This indicates that only a single exponential component is present. Fig. 1 shows the temperature variation of the amplitude of the optical change associated with this relaxation effect. The enthalpy of melting can be calculated from the width of the differential melting curve by using the equations given by Gralla and Crothers (20). In the case of the melting curve shown in Fig. 1, ΔH is calculated to be 15 kcal/mol (1 kcal = 4.184 kJ); generally, we found values in the range 15–20 kcal/mol.

Relaxation Time Is Independent of 5S RNA Concentration. We measured relaxation times of the early melting transition at several 5S RNA concentrations, and found that τ is independent of RNA concentration. This demonstrates that the early melting transition reflects a unimolecular conformational change.

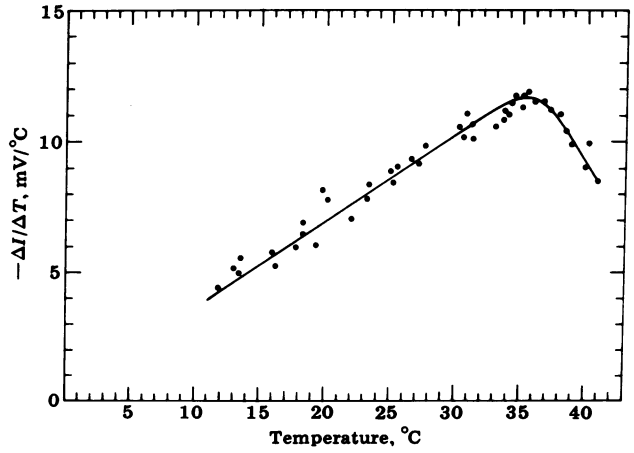

FIG. 1. Differential melting curve for the *E. coli* 5S RNA. The total amplitude ΔI (in mV) was obtained from the zero-time intercept of the semilogarithmic plot and divided by temperature-jump size (3.76°C). The resultant $\Delta I/\Delta T$ was then plotted versus the temperature corresponding to the midpoint of the temperature jump. For each jump, the starting light intensity I was 5000 mV. The absorbance (A_{260}) of the 5S RNA sample in the temperature-jump cell at low temperature was 1.18 in a 1-cm path.

Early Melting Transition Shows Substantial Hyperchromism. The absorbance difference $A_h - A_l$ between high (h)- and low (l)-temperature forms of 5S RNA can be calculated from the equation

$$\frac{1}{I_0}\left(\frac{dI}{dT}\right)_{t_m} = -2.3(A_h - A_l)\frac{\Delta H}{4RT_m^2}, \qquad [1]$$

in which I_0 is the initial intensity of light transmitted by the solution, T is absolute temperature, t_m is the Celsius melting temperature, ΔH is the heat of melting (15–20 kcal/mol), and R is the gas constant. Analysis of the data in Fig. 1 reveals a fractional absorbance increase $(A_h - A_l)/A_l$ of about 0.06. This is about 15% of the 40% hyperchromism expected for melting a fully double helical molecule. Because 5S RNA contains about 120 nucleotides, the absorbance increase in the early melting transition corresponds to the value expected for melting 15% of (120/2) base pairs, or a double helix about 9 base pairs long. Clearly this estimate of the size of the region that melts is much larger than would be obtained from the melting enthalpy.

t_m Decreases with Increasing Salt Concentration and pH. Fig. 2 shows the variation of t_m with Na^+ and Mg^{2+} concentration and with pH. A striking t_m decrease with increasing Na^+ concentration is observed, with a slope of about −54°C per factor of 10 in salt concentration, roughly 3 times larger in magnitude than the 18°C increase per factor of 10 usually found for double helical nucleic acids. The Mg^{2+} concentration dependence is smaller, −13°C per factor of 10, but still substantial. Perhaps most surprisingly, t_m also varies greatly with pH, with an increase of 19°C per 10-fold increase in H^+ concentration.

t_m Variation Implies Proton Release and Counterion Binding upon Melting. The variation of t_m with salt or H^+

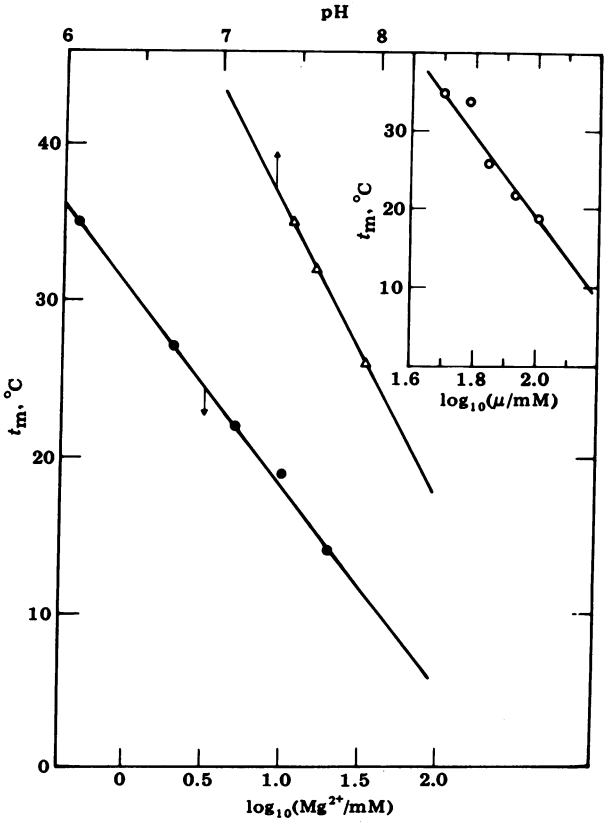

FIG. 2. Dependence of t_m on (*i*) pH (△) (Na^+ = 50 mM, Mg^{2+} = 0.5 mM); (*ii*) the logarithm of Mg^{2+} concentration (●) (Na^+ = 50 mM, pH = 7.45). (*Inset*) Dependence of t_m on the logarithm of the ionic strength μ (○) (Mg^{2+} = 0.5 mM, pH = 7.45).

concentration depends on the enthalpy of melting ΔH and on the difference of salt or H^+ binding by the two forms h and l of native 5S RNA. Assuming no change in anion binding, the dependence can be expressed by the equation (21)

$$\frac{dt_m}{d\ \ln[M]} = -(r_h - r_l)\frac{RT_m^2}{\Delta H}, \qquad [2]$$

in which M can be Na^+, Mg^{2+}, or H^+. The difference in binding $r_l - r_h$ has the following meaning: for each mole of 5S RNA that unfolds, $r_h - r_l = \Delta r$ moles of MX must be added to the solution in order to hold constant the chemical potential of MX, again assuming no change in anion binding.

Analysis of the data in Fig. 2 according to Eq. 2 reveals that $\Delta r = 0.7$ H^+ are released in the low-to-high temperature transition of 5S RNA, whereas $\Delta r = 0.5$ Mg^{2+} are taken up (in 50 mM Na^+) and $\Delta r = 2$ Na^+ (or K^+) are also taken up (in 0.5 mM Mg^{2+}). These results imply that the low-temperature form has a special binding site for $\approx$1 proton, whereas the high-temperature form has higher affinity for counterions, probably because it is more compact and hence has a higher charge density. In addition, Na^+ binding probably compensates H^+ release during melting.

Proton release in the l → h transition is also indicated by the much smaller melting signal seen when Tris is used as buffer. The large heat of protonation of Tris (−11 kcal/mol) nearly compensates the heat of RNA melting, and a broad flat melting curve results.

Calculation of Activation Energies. Activation energies of the melting transition were calculated by assuming a two-state melting transition

$$l \underset{k_R}{\overset{k_D}{\rightleftharpoons}} h, \qquad [3]$$

in which l is the low-temperature form, h is the product of the early melting transition or high-temperature form, and k_D and k_R are rate constants for dissociation and reassociation. For this mechanism, $1/\tau = k_D + k_R$, and the equilibrium constant $K = k_D/k_R$. Knowing ΔH and $K = 1$ at $T = T_m$, K at any temperature T can be calculated from the van't Hoff equation $\partial \ln K/\partial(1/T) = -\Delta H/R$ by integration (assuming ΔH is independent of temperature). From the K value and measured relaxation time at each temperature we then calculated k_D and k_R. A semilogarithmic plot of k_D or k_R against $1/T$ was constructed; its slope multiplied by $-R$ is the Arrhenius activation energy for forward or reverse reactions. These were found to be $E_A^D = 25$ kcal/mol and $E_A^R = 6$–10 kcal/mol, respectively.

Dependence of the Rate Constants on Ion Concentration. The variation of k_D and k_R with ion concentration at constant temperature can be calculated from the equation (22)

$$\left(\frac{\partial \ln k_D}{\partial \ln[M]}\right)_T = -\frac{d \ln \tau_m}{d \ln[M]} + \frac{E_A^D}{R}\left(\frac{d(1/T_m)}{d \ln[M]}\right) \qquad [4]$$

and a corresponding equation relating k_R and E_A^R. In Eq. 4, τ_m is the relaxation time observed at T_m. The variation of $1/T_m$ and the corresponding τ_m values with ln[M] are shown in Figs. 3 and 4. Note that the values of k_R and k_D at T_m can be calculated from the data in Figs. 3 and 4 by using the relationship $1/\tau_m = 2k_R = 2k_D$. Observed values of k_R and k_D at T_m were found to lie in the range 50–2000 s^{-1}, similar to the rate constants for unfolding tRNA tertiary structure (11).

Table 1 summarizes the results obtained by using Eq. 4 to analyze the data in Figs. 3 and 4. Also presented are the average activation parameters found for each set of melting curves. Notice that the difference $(\partial \ln k_D/\partial \ln[M])_T - (\partial \ln k_R/\partial \ln[M])_T$ in Table 1 is, within experimental error, the difference in apparent ion binding Δr.

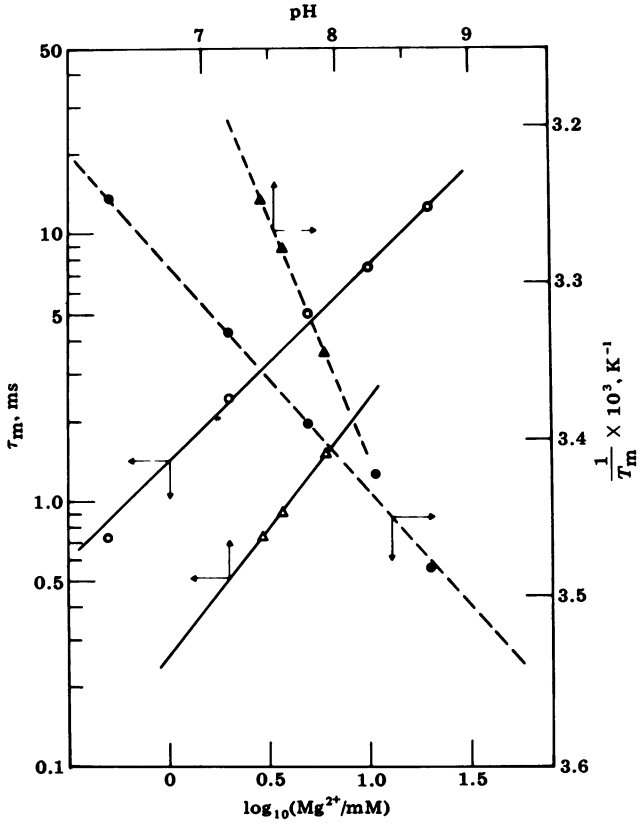

FIG. 3. τ_m (left axis) and reciprocal of absolute melting temperature, T_m (right axis), are plotted vs. (*i*) logarithm of Mg^{2+} concentration (Na^+ = 50 mM, pH = 7.45); (*ii*) pH (Na^+ = 50 mM, Mg^{2+} = 0.5 mM). (Circles indicate Mg^{2+} concentration and triangles indicate pH.) Solid lines refer to the left axis; broken lines refer to the right axis.

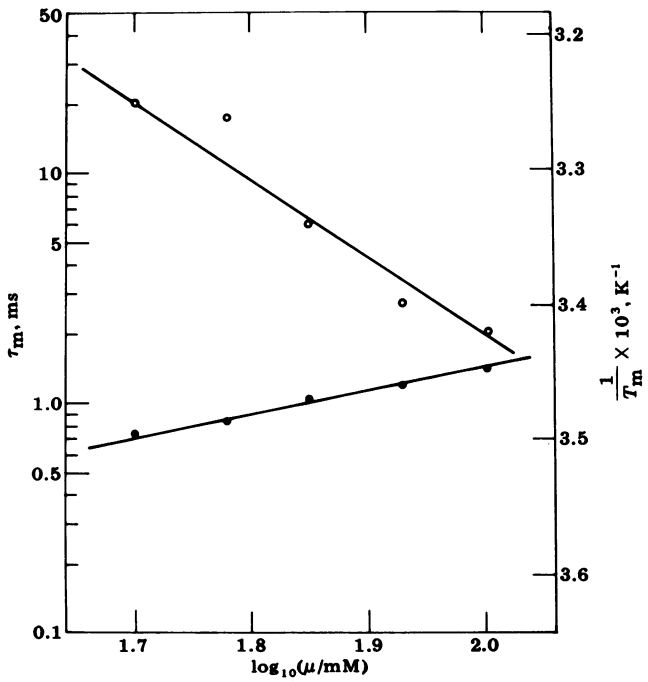

FIG. 4. τ_m (●, left axis) and reciprocal T_m (○, right axis) are plotted vs. logarithm of the ionic strength.

Table 1. Dependence of unfolding dynamics on ion concentration

Ion	$E_A^{D,*}$ kcal/mol	$E_A^{R,*}$ kcal/mol	$\left(\frac{\partial \ln k_D}{\partial \ln[M]}\right)_T$	$\left(\frac{\partial \ln k_R}{\partial \ln[M]}\right)_T$
Mg^{2+}	25	6	0.1	−0.5
Na^+	25	8	2.1	−0.1
H^+	25	10	−0.5	0.2

* Average of activation parameters for each set of melting curves.

Each of the three ions studied acts in a different way. Increase of Mg^{2+} concentration stabilizes the high-temperature form (h) primarily by reducing the rate constant k_R for transforming h to l. In contrast, Na^+ increases the rate constant k_D for dissociation of the low-temperature form.

Increased proton concentration affects both forward and reverse rate constants appreciably, but the main effect seems to be to reduce the rate constant k_D for unfolding the low temperature form. Because the rate constant is roughly proportional to $[OH^-]^{1/2}$, the results are compatible with a mechanism in which OH^--catalyzed removal of a proton contributes to the rate-limiting step in conversion of l to h

$$5S\ RNA(l) + OH^- \underset{k_{21}}{\overset{k_{12}}{\rightleftharpoons}} I + H_2O \xrightarrow{k_{23}} 5S\ RNA(h),$$

in which I is a steady-state intermediate. The nonintegral exponent in the dependence of the rate on $[OH^-]$ indicates that k_{23} and k_{21} are of comparable magnitude in this mechanism. Increase of the cacodylate buffer concentration from 10 to 30 mM did not affect the rate appreciably. However, we have not examined systematically the possible role of general base catalysis in the reaction mechanism.

Addition of Spermidine Further Decreases t_m of the Early Melting Transition. Spermidine, a polyamine with three positive charges at neutral pH, is present in almost all prokaryotic organisms (23). We have checked the effect of spermidine on the early melting transition because of the possible importance of polyamines for the crystallization of *E. coli* 5S RNA, analogous to their role in tRNA crystallization (24, 25). Spermidine, having one more positive charge than Mg^{2+}, should have a greater effect on the early melting transition than Mg^{2+}. The results, as expected, show that addition of 0.1 mM spermidine to the solution containing 50 mM Na^+ and 0.5 mM Mg^{2+} (pH 7.45) reduces t_m from 35 to 29°C, and 0.5 mM spermidine is enough to shift the t_m down to near 0°C.

Difference Spectrum Implies That the Early Melting Region is Approximately 75% A·U Type Stacking Interaction. Fig. 5 shows the absorbance change (measured at 32°C) monitored at wavelengths between 230 nm and 280 nm. According to the parameters of Fresco *et al.* (26), the structure melting is approximately 75% A·U pairs. However, it is not known whether the denaturation spectrum of a tertiary structure with protonated bases will be the same as that of a standard double helix, which is the basis for the parameters used.

Early Melting Transition Is Not the Denaturation Process of Native 5S RNA. We have used gel electrophoresis to monitor the RNA conformational state before and after temperature-jump experiments. The results indicate that the early melting transition does not produce any denatured 5S RNA. Hence we are certain that the transition between l and h forms observed in these studies represents a switch between different conformational states of the native or A form of 5S RNA.

Laser Light Scattering Measurements Indicate That the High-Temperature Form Is Indeed More Compact Than the Low-Temperature Form. We have measured the translational diffusion constant for both the low- and the high-temperature form at 11°C. The solution conditions we chose are (*i*) 30 mM sodium cacodylate, pH 7.0/20 mM $NaClO_4$/0.5 mM $MgCl_2$, (*ii*) 10 mM sodium cacodylate, pH 7.45/300 mM NaCl/10 mM $MgCl_2$. From the measured transition curves, the low-temperature form predominates in solution condition *i* at 11°C, whereas the high-temperature form predominates in solution condition *ii* at 11°C. The diffusion constants, measured at an RNA concentration of A_{260} = 6 and corrected for temperature and solvent viscosity, are $D_{20,w}$ = 5.83 cm^2/s for the low temperature form and $D_{20,w}$ = 6.27 cm^2/s for the high-temperature form. Comparison of these values clearly demonstrates that the high-temperature form is more compact than the low-temperature form, as we also deduced from the dependence of t_m on NaCl concentration.

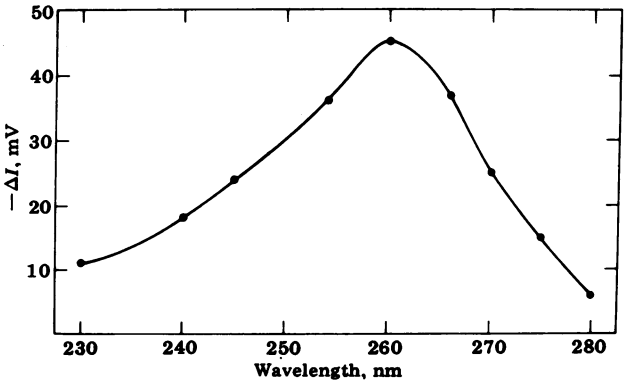

FIG. 5. Thermal difference spectrum of *E. coli* 5S RNA in 30 mM sodium cacodylate, pH 7.45/20 mM $NaClO_4$/0.5 mM $MgCl_2$. Oscilloscope traces of relaxation signals for a temperature jump from 32 to 35.76°C at wavelengths indicated were analyzed. The total amplitudes are plotted against the wavelength. Sample concentration corresponds to A_{260} = 1.36.

DISCUSSION

Early Melting Transition Reflects a Change of Tertiary Structure. Our data strongly favor the involvement of tertiary structure in the early melting transition. First, the enthalpy of the transition, 15–20 kcal/mol, is much smaller than that of any stable double helices. Second, the ratio of absorbance increase to enthalpy change is far larger than observed for double helices. Third, the effect of Mg^{2+} and ionic strength on the t_m of the transition is contrary to that expected for a double helix–coil transition. Fourth, the thermal difference spectrum indicates that approximately 75% A·U pairs are involved in the melting, assuming that the structure is a standard double helix. Inspection of the secondary structure of 5S RNA reveals that no such double helix exists.

Site of Protonation. From our results we cannot tell which bases are involved in the tertiary structural switch, nor can we locate the protonation site. The pH range to which the structure is sensitive (pH 7–8) falls far from the pK_a values of all four constituent bases of 5S RNA, or the internal phosphate or sugar. A possible candidate for the protonation site is the 5′-terminal phosphate, whose pK_a is 6.4. However, we have ruled out this possibility by removal of the 5′-terminal phosphate, using alkaline phosphatase. We not only obtained the same melting curves but also the same pH dependence (results not shown). It seems probable that the strong proton binding results from a tertiary structural interaction that stabilizes hydrogen bonding of a protonated A or C residue, perhaps by salt linkage to phosphate. It may be possible to localize the conformational switch by comparing the nuclease digestion patterns of the two different conformations of native 5S RNA.

It Remains To Be Seen Whether Two Conformational States of 5S RNA Have the Same Affinity Toward the Ribosomal Proteins. 5S RNA is associated with three ribosomal proteins, L5, L18, and L25, in the 50S ribosomal subunit (1). Each protein can be reassociated with 5S RNA *in vitro* in a reconstitution buffer, 10 mM Tris·HCl/300 mM KCl/10 mM $MgCl_2$ (pH 7.6) at 30–37°C. On the basis of our kinetic data, under this reconstitution condition 5S RNA exists in the high-temperature form even at temperatures as low as 0°C. Spierer and Zimmermann (27) have studied the effects of Mg^{2+}, KCl concentration, and pH on the stability of 5S RNA–protein complexes. However, the difference in the binding affinity they observed does not reflect the conformational transition we observed in 5S RNA, because under all the conditions they used we calculate that the RNA existed in the high-temperature (h) form.

Our Results Provide Possible Solution Conditions for Crystallization of Two Conformers of 5S RNA. To our knowledge there has been no success in crystallizing 5S RNA. This may be due to the conformational heterogeneity of 5S RNA under the solution conditions used for crystallization. In the case of yeast $tRNA^{Phe}$, Mg^{2+} and spermine have been shown to be necessary components to crystallize tRNA in both the orthorhombic (24) and the monoclinic forms (25). Likewise, Mg^{2+} and polyamines may be important for crystallizing *E. coli* 5S RNA. We have shown that additions of spermidine, Mg^{2+}, and Na^+ (or K^+) favor the high-temperature form of 5S RNA, whereas addition of H^+ favors the low-temperature form. Therefore, by carefully adjusting the above variables and temperature, one can obtain solution conditions in which either conformer dominates.

Possible Biological Significance. The detailed function of 5S RNA in protein biosynthesis is unknown. Because there is no known function for isolated 5S RNA, we cannot be certain that a conformational switch observed for the RNA in solution is relevant for its properties in the ribosome. However, it seems to us unlikely that a special RNA tertiary structure capable of proton binding at pH 7.5 would arise as a chance artefact. The observed conformational transition has all the desired properties: it is found under near-physiological ionic conditions, it occurs on a millisecond time scale and hence is fast enough to be accommodated as a cyclic process in protein synthesis, the enthalpy change is small enough to make the equilibrium relatively insensitive to temperature change, and, perhaps most importantly, the switch from l to h can be triggered by base catalysis. (In protein synthesis the basic group would presumably be provided by a ribosomal protein.) Finally, the observed change in compaction, 10% change in diffusion constant, is sufficient to provide extensive movement of the kind necessary to shift tRNA and mRNA relative to the ribosome. (A 10% diffusion constant change indicates a ≈15 Å change in dimensions of the elongated 5S RNA molecule.) Hence it seems plausible that a cyclic conformational change of 5S RNA between the l and h forms is an essential part of protein biosynthesis. If so, it should be possible to observe the switch in complexes of 5S RNA with ribosomal proteins, and ultimately in the ribosome itself.

The authors thank Marshal Mandelkern for his assistance in performing laser light-scattering experiments and Dr. Nanibhushan Dattagupta and Daniel Rabin for helpful discussions. We are grateful to Dr. Tom Record for helpful comments. This work was supported by Grant GM 21966 from the National Institutes of Health.

1. Erdmann, V. A. (1976) *Prog. Nucleic Acid Res. Mol. Biol.* **18**, 45–90.
2. Fox, G. & Woese, C. R. (1975) *Nature (London)* **256**, 505–507.
3. Noller, H. F. & Garrett, R. A. (1979) *J. Mol. Biol.* **132**, 621–636.
4. Wagner, R. & Garrett, R. A. (1978) *Nucleic Acid Res.* **5**, 4065–4075.
5. Appel, B., Erdmann, V. A., Stulz, J. & Ackermann, T. (1979) *Nucleic Acid Res.* **7**, 1043–1057.
6. Weidner, H. & Crothers, D. M. (1977) *Nucleic Acids Res.* **4**, 3401–3414.
7. Allen, S. H. & Wong, K. P. (1978) *J. Biol. Chem.* **253**, 8759–8766.
8. Vasiliev, V. D., Selivanova, O. M. & Koteliansky, V. E. (1978) *FEBS Lett.* **95**, 273–276.
9. Stein, A. & Crothers, D. M. (1976) *Biochemistry* **15**, 160–168.
10. Ehrenberg, M., Rigler, R. & Wintermeyer, W. (1979) *Biochemistry* **18**, 4588–4599.
11. Cole, P. E. & Crothers, D. M. (1972) *Biochemistry* **11**, 4368–4374.
12. Crothers, D. M., Cole, P. E., Hilbers, C. W. & Shulman, R. G. (1974) *J. Mol. Biol.* **87**, 63–88.
13. Hilbers, C. W., Robillard, G. T., Shulman, R. G., Blake, R. D., Webb, P. K., Fresco, R. & Riesner, D. (1976) *Biochemistry* **15**, 1874–1882.
14. Staehelin, T., Maglott, D. & Monro, R. E. (1969) *Cold Spring Harbor Symp. Quant. Biol.* **34**, 39–48.
15. Aubert, M., Scott, J. F., Reynier, M. & Monier, R. (1968) *Proc. Natl. Acad. Sci. USA* **61**, 292–299.
16. Crothers, D. M. (1971) in *Procedures in Nucleic Acid Res.*, eds. Cantoni, G. L. & Davies, D. R. (Harper & Row, New York), Vol. 2, pp. 369–388.
17. Marquardt, D. W. (1963) *J. Soc. Ind. Appl. Math.* **11**, 431–441.
18. Dubin, S. B. (1972) in *Methods Enzymol.* **26**, 119–174.
19. Ford, N. C., Jr., Gabler, R. & Karasz, F. (1973) *Adv. Chem. Ser.* **125**, 25–54.
20. Gralla, J. & Crothers, D. M. (1973) *J. Mol. Biol.* **73**, 497–511.
21. Record, M. T., Lohman, T. & Haseth, P. (1976) *J. Mol. Biol.* **107**, 145–158.
22. Yang, S. K. & Crothers, D. M. (1972) *Biochemistry* **11**, 4375–4381.
23. Tabor, C. W. & Tabor, H. (1976) *Annu. Rev. Biochem.* **45**, 285–306.
24. Kim, S. H., Quigley, G., Suddath, F. L. & Rich, A. (1971) *Proc. Natl. Acad. Sci. USA* **68**, 841–845.
25. Ladner, J. E., Finch, J. T., Klug, A. & Clark, B. F. C. (1972) *J. Mol. Biol.* **72**, 99–101.
26. Fresco, J. R., Klotz, L. C. & Richards, E. G. (1963) *Cold Spring Harbor Symp. Quant. Biol.* **28**, 83–90.
27. Spierer, P. & Zimmermann, R. A. (1978) *Biochemistry* **13**, 2474–2479.